

See discussions, stats, and author profiles for this publication at: <https://www.researchgate.net/publication/49632026>

# The functional valency of dodecamannosylated fullerenes with Escherichia coli FimH – Towards novel bacterial antiadhesives

ARTICLE *in* CHEMICAL COMMUNICATIONS · JANUARY 2011

Impact Factor: 6.83 · DOI: 10.1039/c0cc04468g · Source: PubMed

CITATIONS

54

READS

61

8 AUTHORS, INCLUDING:



**Maxime Durka**

devan chemicals

14 PUBLICATIONS 212 CITATIONS

SEE PROFILE



**Joemar Taganna**

NanoTechGalaxy, Inc.

4 PUBLICATIONS 101 CITATIONS

SEE PROFILE



**Julie Bouckaert**

Université des Sciences et Technologies de ...

86 PUBLICATIONS 2,259 CITATIONS

SEE PROFILE

# The functional valency of dodecamannosylated fullerenes with *Escherichia coli* FimH—towards novel bacterial antiadhesives†

Maxime Durka,<sup>a</sup> Kevin Buffet,<sup>a</sup> Julien Iehl,<sup>b</sup> Michel Holler,<sup>b</sup> Jean-François Nierengarten,<sup>\*b</sup> Joemar Taganna,<sup>c</sup> Julie Bouckaert<sup>\*c</sup> and Stéphane P. Vincent<sup>\*a</sup>

Received 17th October 2010, Accepted 28th October 2010

DOI: 10.1039/c0cc04468g

Fullerene hexakis-adducts bearing 12 peripheral mannose moieties have been prepared by grafting sugar derivatives onto the fullerene core and assayed as inhibitors of FimH, a bacterial adhesin, using isothermal titration calorimetry, surface plasmon resonance and hemagglutination assays.

The emerging resistance of most pathogenic bacteria to clinically relevant antibiotics urges the scientific community to find a new class of molecules or a new mode of actions to treat infectious diseases. Antivirulence has recently emerged as an alternative antibacterial chemotherapeutic strategy to the discovery of new bactericides or bacteriostatic molecules.<sup>1</sup> Indeed, innovative approaches should arise from targeting the bacterial functions that contribute to the infection and lead the pathogen to cause damage in a host. Different virulence mechanisms that allow pathogenic bacteria to invade, to disseminate and adapt in the host have been evidenced. With the antivirulence concept in mind, we have recently reported on the inhibition of heptosyltransferases as a novel approach to inhibit the bacterial cell wall resistance to innate immune response.<sup>2,3</sup> As part of this research, we now report on fullerene-sugar balls<sup>4</sup> designed for a complementary antivirulence approach: the prevention of colonization and bacterial adhesion to host cells. Indeed, bacterial adhesion to cell surface tissues is one of the very first steps of the infective process and is often mediated by carbohydrate–protein interactions. This is the case of the uropathogenic strain of *E. coli* that causes urinary tract infections.<sup>5</sup> This bacterium exploits FimH, an adhesin overexpressed at the tip of pili, to bind terminal mannose moieties found at the surface of the host epithelial cells.<sup>6</sup> The multivalent presentation of carbohydrates is generally an essential point for achieving high affinity interactions with lectins<sup>7,8</sup> and different synthetic scaffolds allowing a multivalent presentation of mannosyl ligands have been already assayed against FimH using either surface plasmon resonance (SPR),<sup>9</sup> ELISA<sup>10</sup> or

inhibition of hemagglutination and bladder cell assay.<sup>11</sup> The level of inhibition or binding was found to be highly dependent on the number of mannoside residues and the nature of the spacer. A direct relationship between these factors has however not been clearly addressed so far. In this communication, we now elucidate this critical point by a unique combination of three experimental techniques: isothermal titration calorimetry (ITC), SPR and hemagglutination assays. We also show the ability of the fullerene-based globular glycoconjugates to aggregate FimH, a key issue in view of developing antiadhesive molecules. One of the most important questions that we addressed was thus to determine the functional valency of the multimers we synthesized, in other words the number of adhesins that can bind the dodecaglycosylated fullerenes.

For this study, we designed fullerene sugar balls 1–3 (Fig. 1) displaying twelve peripheral mannose residues. Fullerene hexakis-adducts 1 and 2 were prepared in four steps using the methodology we recently described.<sup>4</sup>

As demonstrated by Roy *et al.*, the presence of an aromatic residue properly positioned in the spacer between the carbohydrate unit and the central scaffold of the multivalent platform may dramatically affect the binding properties of the multimers towards adhesins.<sup>9</sup> Thus, we designed and synthesized fullerene 3 which bears a benzylic aromatic ring

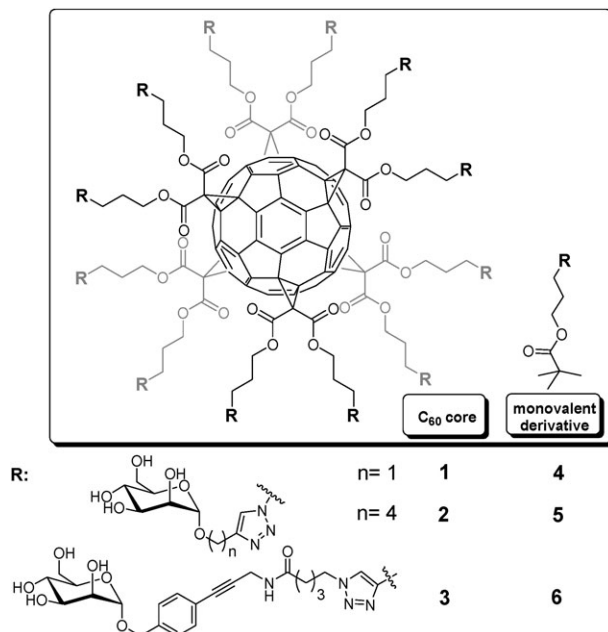


Fig. 1 Fullerene sugar balls 1–3 and the corresponding monovalent model compounds 4–6.

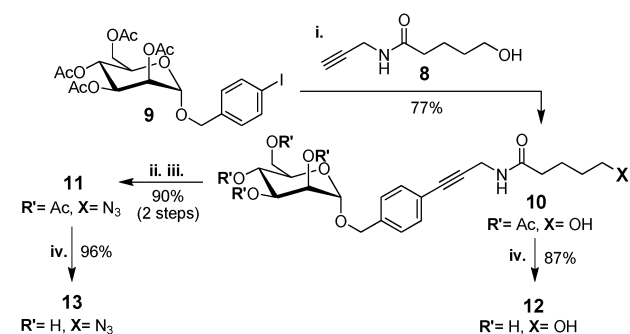
<sup>a</sup> University of Namur (FUNDP), Département de Chimie, Laboratoire de Chimie Bio-Organique, rue de Bruxelles 61, B-5000 Namur, Belgium. E-mail: stephane.vincent@fundp.ac.be

<sup>b</sup> Laboratoire de Chimie des Matériaux Moléculaires, Université de Strasbourg et CNRS (UMR 7509), Ecole Européenne de Chimie, Polymères et Matériaux (ECPM), 25 rue Becquerel, 67087 Strasbourg Cedex 2, France.

E-mail: nierengarten@chimie.u-strasbg.fr

<sup>c</sup> Structural Biology Brussels at the Vrije Universiteit Brussel, VIB, Pleinlaan 2, 1050 Brussels, Belgium. E-mail: bouckaetj@vub.ac.be

† Electronic supplementary information (ESI) available: Experimental details for the ITC experiments, the hemagglutination assays, and for the preparation of the new compounds. See DOI: 10.1039/c0cc04468g



**Scheme 1** Reagents and conditions: (i) **8**, Pd(PPh<sub>3</sub>)<sub>2</sub>Cl<sub>2</sub>, CuI, NEt<sub>3</sub>, DMF, m.w., 6 min; (ii) MsCl, DMAP, Py, 45 min, RT; (iii) NaN<sub>3</sub>, DMF, 2 h, 60 °C; (iv) MeONa, MeOH, 15 min, 0 °C to RT.

at the anomeric position and an amide group that might provide favorable contacts with the lectin binding cavity, as expected from the FimH 3D structure.<sup>12</sup> The key intermediate **13** bearing an azide functionality was prepared by a Sonogashira cross-coupling reaction between alkyne **8** and mannoside **9** in 77% yield (Scheme 1). The former was easily prepared from D-mannose peracetate and iodobenzyl alcohol under standard conditions. Intermediate **10** was deprotected to give the monomeric mannoside **12** which served as a reference for the biological evaluations. The same intermediate **10** was transformed into the desired deprotected azide **13**, through a sequence of mesylation, azidation and Zemplén deprotection. Finally, we coupled azide **13** with the fullerene bearing twelve alkyne functionalities. The structure of compound **3** was confirmed by its <sup>1</sup>H and <sup>13</sup>C NMR spectra.

The binding affinities of compounds **1–6**, and **12** for FimH were determined by ITC. The latter is an important technique because it provides the stoichiometry of the binding process and a true view of the equilibrium affinity. To the best of our knowledge, this study represents the first ITC experiments reported on FimH to date. The results are summarized in Table 1. The comparison of fullerenes **1** and **2** clearly shows that increasing the distance between the mannose residues and the fullerene core improved significantly the binding affinities. Interestingly, the ITC allowed us to determine the number *N* of carbohydrates that can bind the lectin. Therefore, the value 1/*N* (Table 1) represents the number of lectins that can bind to the glycosylated fullerene. Here again, the spacer length plays a significant role since around 4 mannose units from fullerene **1** effectively bind FimH whereas fullerene **2**, with a longer spacer,

allows the binding of roughly 6 mannose moieties. Fullerenes **1** and **2** displayed similar dissociation constants than their corresponding monomers **4** and **5**, respectively. The analysis of the thermodynamic data showed that displaying the mannose residues around the fullerene core structure is favourable for the enthalpic contribution. On the other hand, the binding affinities were hampered by a significant entropic cost, as observed for other lectins such as ConA.<sup>13</sup>

This entropic cost and the difference in binding properties of sugar balls **1** and **2** could be explained by the structure of FimH itself. Contrary to most other lectins, FimH displays a deep and narrow binding pocket. The mannose residues have to reach the bottom of this cavity to properly bind the lectin. Thus, the fullerene core structure has to approach the protein surface, as shown in the model structure provided in the ESI.† We then turn our attention to fullerene **3** bearing a benzyl moiety linked to each mannose unit. Due to its hydrophobic nature, this fullerene was not fully soluble at the highest concentrations required for the ITC experiments and the hemagglutination assays. Therefore, all the ITC experiments have been performed with 5% DMSO to allow a comparison with fullerenes **1** and **2**. An unexpected phenomenon occurred during both the usual titration of FimH by **3** and the reverse titration mode (titration of **3** with FimH). Instead of the typical sigmoidal plot, we observed a first binding event followed by a strong exothermic jump that could be attributed to an aggregation of the protein during the experiment. Given the fact that the fullerene was totally soluble under these conditions and that FimH did not aggregate with compounds **1–2**, **4–6** and **12**, we can safely conclude that multimer **3** itself triggered the aggregation of FimH. From the first binding event observed in the ITC plot, the aggregation begins when 5 to 6 mannose residues are bound to FimH.

This specific phenomenon is indeed interesting since, from a therapeutic point of view, such an aggregation process could be advantageous in a strategy dedicated to preventing bacterial colonizations. The fact that the molarity observed for the aggregation of FimH with fullerene **3** is roughly the same as the molar ratio calculated for fullerene **2** strongly suggests that the two processes (binding and aggregation) are linked.

To determine the binding affinity of fullerene **3**, we inhibited in solution the binding of FimH to a mannose-functionalized sensor chip by the addition of fullerene **3** and measured SPR on a Biacore3000. The binding affinity of the whole series of molecules is reported in Table 1. Importantly, the data

**Table 1** FimH relative affinities of mannosylated fullerenes as determined by ITC and SPR

Ligand	ITC <sup>d</sup>				SPR	
	Δ <i>H</i> /kJ mol <sup>−1</sup>	Δ <i>S</i> /J mol <sup>−1</sup> K <sup>−1</sup>	<i>K</i> <sub>d</sub> /nM	1/ <i>N</i> <sup>a</sup>	<i>K</i> <sub>d</sub> /nM	<i>N</i> <sup>c</sup>
<b>1</b>	−238.28 ± 3.31	−674	95 ± 8	3.89	39.8 ± 2.0	3.4
<b>2</b>	−444.92 ± 6.64	−1360	26 ± 2	6.53	12.3 ± 1.2	7
<b>3</b>	ND <sup>b</sup>	ND <sup>b</sup>	ND <sup>b</sup>	ND <sup>b</sup>	8.9 ± 1.1	7
<b>4</b>	−43.07 ± 3.91	−11	92 ± 6	1.04	70.0 ± 2.7	—
<b>5</b>	−61.19 ± 0.28	−60	20 ± 2	1.06	10.7 ± 1.6	—
<b>6</b>	−46.67 ± 0.65	−30	30 ± 1	0.95	9.2 ± 1.1	—
<b>12</b>	−47.76 ± 0.33	−20	40 ± 3	0.97	32.9 ± 3.2	—

<sup>a</sup> 1/*N* represents the number of lectin molecules that can bind the fullerene. <sup>b</sup> ND: not determined; the complete plot could not be obtained due to the aggregation. <sup>c</sup> Effective D-mannose units as evaluated from Fig. 2: best fitting of χ<sup>2</sup> vs. *n* in SPR measurements. <sup>d</sup> Δ*H* and Δ*S* values refer to the global multimer/protein association.

deduced from the SPR measurements were in good agreement with those obtained by ITC (Table 1). The  $K_d$  values of fullerenes **1**, **2** and **3** compare well with those of the best multimeric mannoses reported to date in the literature (0.45 to 273 nM), as measured by SPR.<sup>9</sup>

For monomers **4**, **5**, **6** and **12**, the fitting using the solution affinity interaction model worked properly and provided  $K_d$  values in the nanomolar range. However, the same equation did not allow a correct fitting for fullerenes **1**, **2** and **3** (see ESI†). To obtain a better fit of the SPR solution affinity between FimH and the fullerenes, we substituted the fullerene concentrations by the “effective mannose concentration”, by multiplying the fullerene concentration with the number  $n$  of mannose units accessible to the FimH adhesin, and evaluated the evolution of  $\chi^2$  versus  $n$  (Fig. 2). Excellent fits were achieved with a number of effective mannose units,  $n$ , almost identical to the functional valency,  $1/N$ , from the calorimetric data (Table 1). The  $K_d$  values reported in Table 1 thus correspond to the dissociation constant of one functional mannose subunit as part of the whole fullerene structure. SPR thus confirmed the ITC findings that the fullerenes can accommodate four FimH molecules for the shortest spacer and up to seven lectins for fullerenes **2** and **3**. In conclusion, the functional valencies of the fullerenes ( $1/N$  in Table 1), directly measured using ITC, could be readily applied to the molar concentrations of the multivalent glycoconjugates to correspond to the SPR solution affinity model.

Contrary to many plant and bacterial lectins that are multimeric and may give rise to huge multivalent effects, FimH is a monomeric adhesin for which multivalent effects are not expected as a purified protein. However, as mentioned by Roy *et al.*<sup>9</sup> and Heidecke and Lindhorst,<sup>10</sup> the average binding strength per mannose unit of multimers (such as fullerenes **1**, **2** and **3**) compared to methyl- $\alpha$ -D-mannose ( $K_d = 2.2 \mu\text{M}$ )<sup>12</sup> is apparently greatly enhanced. Our data however clearly show that the length and the structure of the anomeric substituent are the key factors to dramatically enhance the binding affinity of the carbohydrate subunit rather than multivalent effects.

On the other hand, multivalent effects may be expected by the presentation of FimH on type-1 fimbriae of bacteria.<sup>7,14</sup>

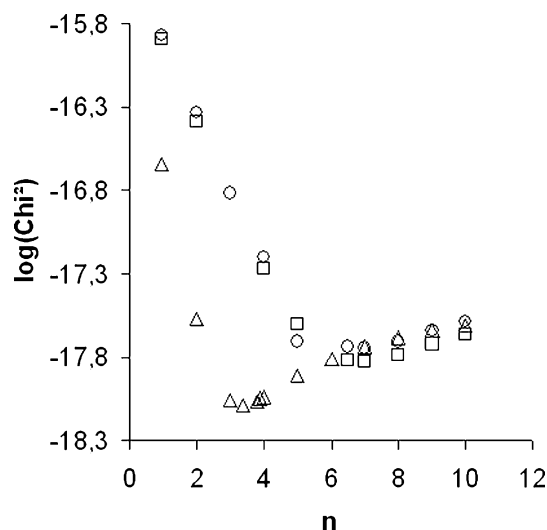


**Fig. 2** Evaluation of the number  $n$  of effective ligands per fullerene using SPR. Fullerene **1** =  $\Delta$ ; **2** =  $\square$ ; **3** =  $\circ$ .

**Table 2** Inhibition of hemagglutination (HAI)

Ligand	<b>4</b>	<b>1</b>	<b>5</b>	<b>2</b>	<b>12</b>	<b>3</b>
Titer <sup>a</sup> /μM	100	3.4	6.6	1.5	29.5	10.4
Ratio <sup>b</sup> m/D		30		4.4		2.8

<sup>a</sup> HAI were performed in phosphate buffer with 10% DMSO. <sup>b</sup> Ratio: monomer titer (m)/corresponding dodecamer titer (D).

Therefore, the inhibitory capacities of the fullerenes with *E. coli* UTI89 were evaluated in a hemagglutination inhibition assay (HAI). Addition of bacteria to guinea pig erythrocytes produces a cross-linked matrix due to interaction of FimH with the glycocalyx of the red blood cells. Subsequent additions of the fullerenes into the wells eventually prevented the agglutination reaction. The inhibition titer is defined as the lowest concentration of the glycoconjugate at which hemagglutination is still inhibited (Table 2).

Under those conditions, all the fullerene derivatives displayed a low micromolar inhibition level, in each case lower than their corresponding monomer. A clear multivalent effect was only evidenced with fullerene **1** which has an inhibition titer 30-fold lower (*ca.* 3-fold per mannose residue) than its corresponding monomer **4**.

In conclusion, we have reported on the synthesis of fullerene glycoconjugates that were assessed as ligand of the bacterial adhesin FimH. Low nanomolar affinities levels were measured by ITC and SPR. Most importantly, the number of possible interactions between the multimers and the lectin and the average binding strength per functional mannose unit could be measured. Thus, we proved, for the first time, that a globular C<sub>60</sub> structure can accommodate up to 7 FimH molecules. The functional valency of these fullerenes could be assessed by the unique comparison of two complementary techniques.

This work was supported by FNRS (FRFC grant 2.4.625.08.F) and a RTN grant (2005–019561).

## Notes and references

- S. Eisaich, *Curr. Opin. Chem. Biol.*, 2008, **12**, 400–408.
- H. Dohi, R. Périon, M. Durka, M. Bosco, Y. Roué, F. Moreau, S. Grizot, A. Ducruix, S. Eisaich and S. P. Vincent, *Chem.–Eur. J.*, 2008, **14**, 9530–9539.
- S. Grizot, M. Salem, V. Vongsouthi, L. Durand, F. Moreau, H. Dohi, S. Vincent, S. Eisaich and A. Ducruix, *J. Mol. Biol.*, 2006, **363**, 383–394.
- J. F. Nierengarten, J. Iehl, V. Oerthel, M. Holler, B. M. Illescas, A. Munoz, N. Martin, J. Rojo, M. Sanchez-Navarro, S. Cecioni, S. Vidal, K. Buffet, M. Durka and S. P. Vincent, *Chem. Commun.*, 2010, **46**, 3860–3862.
- A. Wellens, C. Garofalo, H. Nguyen, N. Van Gerven, R. Slattegard, J. P. Hernalsteens, L. Wyns, S. Oscarson, H. De Greve, S. Hultgren and J. Bouckaert, *PLoS One*, 2008, **3**, e2040.
- J. Bouckaert, *et al.*, *Mol. Microbiol.*, 2006, **61**, 1556–1568.
- R. J. Pieters, *Org. Biomol. Chem.*, 2009, **7**, 2013–2025.
- J. J. Lundquist and E. J. Toone, *Chem. Rev.*, 2002, **102**, 555–578.
- M. Touaibia, A. Wellens, T. C. Shiao, Q. Wang, S. Sirois, J. Bouckaert and R. Roy, *ChemMedChem*, 2007, **2**, 1190–1201.
- C. D. Heidecke and T. K. Lindhorst, *Chem.–Eur. J.*, 2007, **13**, 9056–9067.
- S. G. Gouin, A. Wellens, J. Bouckaert and J. Kovensky, *ChemMedChem*, 2009, **4**, 749–755.
- J. Bouckaert, J. Berglund, M. Schembri, E. De Genst, L. Cools, M. Wuhrer and C. S. Hung, *et al.*, *Mol. Microbiol.*, 2005, **55**, 441–455.
- T. K. Dam and C. F. Brewer, *Methods Enzymol.*, 2004, **379**, 107–128.
- A. Imbert, Y. M. Chabre and R. Roy, *Chem.–Eur. J.*, 2008, **14**, 7490–7499.